

## Role of valence-band Co 3d states on ferromagnetism in Zn<sub>1-x</sub>Co<sub>x</sub>O nanorods

J. W. Chiou, H. M. Tsai, C. W. Pao, K. P. Krishna Kumar, J. H. Chen, D. C. Ling, F. Z. Chien, and W. F. Pong<sup>a)</sup>

Department of Physics, Tamkang University, Tamsui 251, Taiwan

M.-H. Tsai

Department of Physics, National Sun Yat-Sen University, Kaohsiung 804, Taiwan

J. J. Wu, M.-H. Yang, and S. C. Liu

Department of Chemical Engineering, National Cheng Kung University, Tainan 701, Taiwan

I.-H. Hong,<sup>b)</sup> C.-H. Chen, H.-J. Lin, and J. F. Lee

National Synchrotron Radiation Research Center, Hsinchu 300, Taiwan

(Received 30 October 2006; accepted 13 December 2006; published online 5 February 2007)

This work investigates the electronic and ferromagnetic properties of Zn<sub>1-x</sub>Co<sub>x</sub>O nanorods using x-ray absorption, x-ray magnetic circular dichroism, and scanning photoelectron microscopy methods. The magnetic moment of Co ions in Zn<sub>1-x</sub>Co<sub>x</sub>O nanorods is found greatly reduced relative to that of the Co metal. The intensities of valence-band features near the valence-band maximum/Fermi level ( $E_F$ ) of ferromagnetic nanorods are substantially larger than those of weaker ferromagnetic nanorods, suggesting that the occupation of near- $E_F$  valence-band Co 3d states is important in determining the ferromagnetic behavior in Zn<sub>1-x</sub>Co<sub>x</sub>O nanorods. © 2007 American Institute of Physics. [DOI: [10.1063/1.2432234](https://doi.org/10.1063/1.2432234)]

Dilute magnetic semiconductors<sup>1</sup> (DMSs) have been intensively investigated because they have a great potential for use as spintronic materials.<sup>2</sup> Transition metal (TM)-doped ZnO is of particular interest because its Curie temperature exceeds room temperature, so that it can be used in practical devices.<sup>3</sup> UV lasing at room temperature has been observed in highly oriented ZnO nanorods.<sup>4</sup> TM-doped ZnO nanorods, with a combination of excellent room-temperature ferromagnetic and optical properties, have attracted much interest in versatile functional nano-spintronic-device applications. However, ferromagnetism (FM) depends strongly on the sample preparation condition<sup>5</sup> and the nature of FM in DMSs remains controversial.<sup>6,7</sup> Various theoretical models<sup>3,8-10</sup> have been proposed to understand FM in DMSs. Thin film and polycrystalline Zn<sub>1-x</sub>M<sub>x</sub>O ( $M$ =Mn and/or Fe, Co) samples have been studied using x-ray absorption<sup>11-14</sup> and photoemission spectroscopy.<sup>12,15</sup> Recently, highly oriented ZnO,<sup>16,17</sup> Zn<sub>1-x</sub>Co<sub>x</sub>O, and Zn<sub>1-x</sub>Mg<sub>x</sub>O (Ref. 18) nanorods have been studied by Chiou *et al.* using x-ray absorption near-edge structure (XANES) and scanning photoelectron microscopy (SPEM). Here, a combination of XANES, x-ray magnetic circular dichroism (XMCD), and SPEM measurements was performed for ferromagnetic and weak ferromagnetic types of Zn<sub>1-x</sub>Co<sub>x</sub>O nanorods to better understand the role of Co 3d states in influencing the ferromagnetic properties of Co-doped ZnO.

Room-temperature O  $K$ - and Co  $L_{3,2}$ -edge XANES, Co  $L_{3,2}$ -edge XMCD, and SPEM measurements were performed at the National Synchrotron Radiation Research Center in Hsinchu, Taiwan. Highly oriented Zn<sub>1-x</sub>Co<sub>x</sub>O nanorods and

reference ZnO ( $x=0$ ) were deposited on the Si substrate using chemical vapor deposition method. The  $x=0.057$  and  $0.078$  nanorods were grown at a temperature of  $525^\circ\text{C}$ , while  $x=0.061$  and  $0.082$  nanorods were grown at  $500^\circ\text{C}$ . Details of the preparation and characterization of the Zn<sub>1-x</sub>Co<sub>x</sub>O nanorods have been presented elsewhere.<sup>19</sup> Scanning electron microscope (SEM) and high-resolution transmission electron microscope (TEM) measurements revealed that Zn<sub>1-x</sub>Co<sub>x</sub>O and ZnO nanorods were approximately  $540\pm 50$  nm long and  $80\pm 20$  nm in diameter, as shown in the inset of Fig. 1.

Figure 1 presents x-ray diffraction (XRD) spectra of Zn<sub>1-x</sub>Co<sub>x</sub>O and ZnO nanorods and the reference CoO powder and Co metal (the intensity in log unit). Zn<sub>1-x</sub>Co<sub>x</sub>O nanorods have a predominant reflection of (002) at  $\sim 34.2^\circ$ , indicating that Co doping does not alter the ZnO hexagonal (wurtzite) structure. XRD spec-

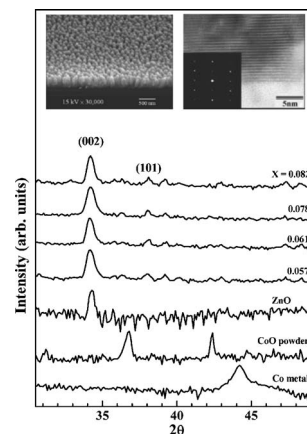


FIG. 1. (a) XRD measurements of well-aligned Zn<sub>1-x</sub>Co<sub>x</sub>O and ZnO nanorods and the reference CoO powder and Co metal (the intensity in log unit). The insets show representative SEM and TEM images and the corresponding electron diffraction from Zn<sub>1-x</sub>Co<sub>x</sub>O ( $x=0.057$ ) nanorods.

<sup>a)</sup> Author to whom correspondence should be addressed; electronic mail: [wfpong@mail.tku.edu.tw](mailto:wfpong@mail.tku.edu.tw)

<sup>b)</sup> Permanent address: Department of Applied Physics, National Chiayi University, Chiayi, Taiwan.

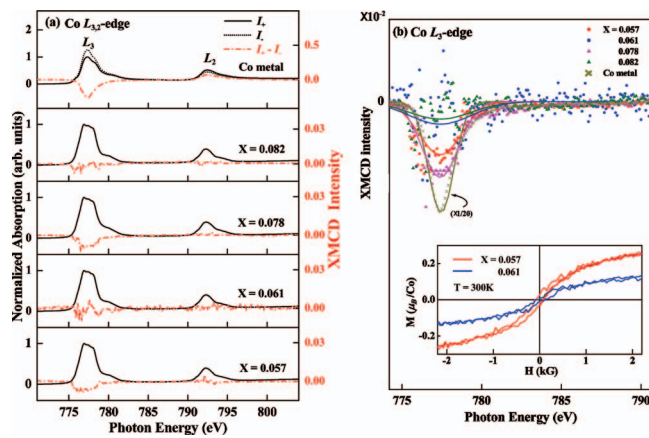


FIG. 2. (Color) (a) Normalized Co  $L_{3,2}$ -edge XANES and XMCD spectra of  $Zn_{1-x}Co_xO$  nanorods and the reference Co metal. (b) Magnified view of XMCD features of  $Zn_{1-x}Co_xO$  nanorods and the reference Co metal at the Co  $L_3$  edge. (The intensity of Co metal has been scaled by a factor of  $1/20$ .) The inset plots hysteresis loops of  $Zn_{1-x}Co_xO$  nanorods with  $x=0.057$  and  $0.061$  at room temperature.

tra of  $Zn_{1-x}Co_xO$  nanorods do not exhibit any Bragg peaks of CoO and Co metals which excludes CoO crystallite phase segregation and formation of Co clusters/precipitates in  $Zn_{1-x}Co_xO$  nanorods. However, XRD measurements cannot exclude the existence of the amorphous CoO phase.<sup>20</sup> Structural characterization of  $Zn_{1-x}Co_xO$  nanorods has also been performed using high-resolution TEM. The analyses of the bottom, middle, and top regions of those nanorods show the absence of segregated clusters of impurity phase throughout the nanorods, indicating that  $Zn_{1-x}Co_xO$  nanorods have mainly a single-phase structure.

Figure 2(a) presents normalized Co  $L_{3,2}$ -edge XANES and XMCD (i.e.,  $I_+ - I_-$ ) spectra of  $Zn_{1-x}Co_xO$  nanorods and the reference Co metal.  $I_+$  ( $I_-$ ) refers to the absorption spectrum obtained by projecting the spin of the incident photons parallel (antiparallel) to the spin direction of the Co  $3d$  majority-spin states. The general line shapes of the Co  $L_{3,2}$ -edge XANES spectra are very similar to those of polycrystalline  $Zn_{1-x}Co_xO$  samples, reported by Wi *et al.*<sup>12</sup> The XMCD spectra of  $Zn_{1-x}Co_xO$  nanorods show the presence of a magnetic moment, though they differ noticeably from those of the Co metal. Figure 2(b) displays the smoothly fitted curves of the noisy magnified Co  $L_3$ -edge negative XMCD data, which suggests that the nanorods ( $x=0.057$  and  $0.078$ ) prepared at a higher temperature ( $525^\circ\text{C}$ ) have larger magnetic moments than those ( $x=0.061$  and  $0.082$ ) prepared at a lower temperature ( $500^\circ\text{C}$ ). The lower inset of Fig. 2(b) shows the magnetization hysteresis loops ( $M$ - $H$  curves) of the  $x=0.057$  and  $0.061$  nanorods, respectively, which illustrates that both samples are ferromagnetic at room temperature and the one grown at  $525^\circ\text{C}$  has a larger magnetic moment in consistent with the XMCD result. The magnetic moments of the Co ions in  $Zn_{1-x}Co_xO$  nanorods can be estimated from the saturation of the  $M$ - $H$  curves to be  $\sim 0.4\mu_B/\text{Co}$  for  $x=0.057$  and  $0.2\mu_B/\text{Co}$  for  $x=0.061$  with magnetic fields up to 1 T (not fully shown), which are about 23% and 13% of that of the Co atom in the Co metal ( $1.7\mu_B/\text{Co}$ ),<sup>6</sup> respectively. The reduction of the Co magnetic moment in  $Zn_{1-x}Co_xO$  nanorods relative to that of the Co metal can be interpreted due to hybridization with the O  $2p$  orbitals that delocalize Co  $3d$  orbitals and can also be due to geometrical frustration of the wurtzite ZnO matrix, which

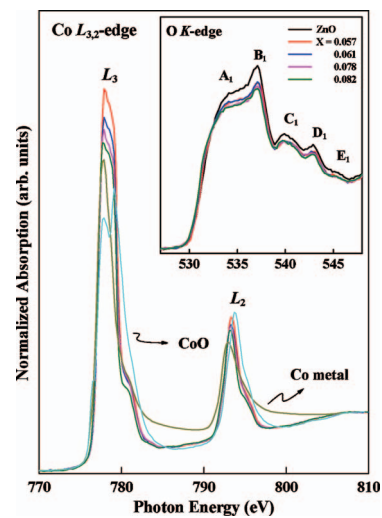


FIG. 3. (Color) Co  $L_{3,2}$ -edge XANES spectra of  $Zn_{1-x}Co_xO$  and ZnO nanorods and the reference CoO and Co metal. The inset shows the O  $K$ -edge XANES spectra of the  $Zn_{1-x}Co_xO$  and ZnO nanorods.

results in imperfect alignment of the spin moments of Co  $3d$  electrons.

Figure 3 shows that the intensities of white-line features at the Co  $L_{3,2}$  edge decrease monotonically with  $x$ . This trend suggests that the occupation of the Co  $3d$  states increases as the Co concentration increases of  $Zn_{1-x}Co_xO$  nanorods. The O  $K$ -edge spectra in the inset of Fig. 3 show that the intensities of XANES features  $A_1$ – $E_1$  of  $Zn_{1-x}Co_xO$  nanorods are nearly identical but smaller than those of ZnO nanorods. In contrast, the O  $K$ -edge XANES spectra of the ferromagnetic Co-doped ZnO films obtained recently by Krishnamurthy *et al.* have somewhat different line shapes and have additional features relative to those of undoped film, which was interpreted by hybridization between O  $2p$  and Co  $3d$  and oxygen vacancies.<sup>14</sup> Since features  $A_1$ – $E_1$  are associated with electron excitations from O  $1s$  to  $2p_{\sigma}$  (along the bilayer) and O  $2p_{\pi}$  (along the  $c$  axis) states,<sup>16–18</sup> this suggests that the occupation of O  $2p$  derived states is enhanced through Co  $3d$ -O  $2p$  hybridization.

Figure 4 displays spatially resolved valence-band photo-

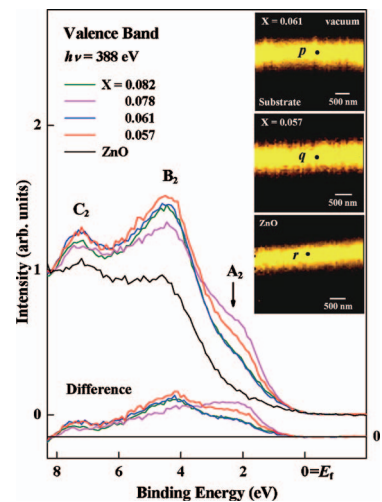


FIG. 4. (Color) Valence-band photoemission spectra obtained from selected positions  $p$ ,  $q$ , and  $r$  in Zn  $3d$  SPEM cross-sectional images of well-aligned  $Zn_{1-x}Co_xO$  ( $x=0.061$  and  $0.057$ ) and ZnO nanorods. The lower inset plots difference valence-band spectra between  $Zn_{1-x}Co_xO$  and ZnO nanorods.

emission spectra of  $\text{Zn}_{1-x}\text{Co}_x\text{O}$  and ZnO nanorods. The Zn 3d SPEM images in the insets show cross-sectional views of nanorods with  $x=0$ , 0.057, and 0.061, in which the bright areas have maximum Zn 3d intensities. Figure 4 shows photoelectron yields from the selected positions in the sidewall regions of  $\text{Zn}_{1-x}\text{Co}_x\text{O}$  nanorods with  $x=0.061$ , 0.057, and 0.0 indicated by  $p$ ,  $q$ , and  $r$  in the images. The zero energy refers to the valence-band maximum (VBM), which is the threshold of the emission spectrum and is also the Fermi level ( $E_F$ ). The spectra exhibit two main features,  $B_2$  and  $C_2$ . Feature  $B_2$  is dominated by occupied O 2p states and feature  $C_2$  is associated with the O 2p and Zn 3d/4sp hybridized states of ZnO nanorods.<sup>16–18</sup> This figure generally shows that the intensities of features  $B_2$  and  $C_2$  are enhanced with the Co doping. The smaller shoulder,  $A_2$ , at  $\sim 2$  eV below  $E_F$  is attributable to the Co 3d partial density of states (DOSs) inferred by band structure calculations,<sup>15,21</sup> which can also be inferred from the comparison of the valence-band photoemission spectra of pure ZnO and  $\text{Zn}_{1-x}\text{Co}_x\text{O}$  nanorods shown in Fig. 4 and of  $\text{Zn}_{1-x}\text{Co}_x\text{O}$  and  $\text{Zn}_{1-x}\text{Mg}_x\text{O}$  nanorods of Ref. 18, which shows Mg doping does not increase the DOSs near  $E_F$ . Since deep-defect and dangling-bond or surface states usually lie in the vicinity of  $E_F$ , these states can also contribute to feature  $A_2$ . The monotonically decrease of the intensity of the Co  $L_{3\text{-edge}}$  XANES white-line feature shown in Fig. 3 with the Co content suggests an increase of the Co 3d-orbital occupation with the Co content. However, the intensity of feature  $A_2$  does not show the trend of  $I(0.082) > I(0.078) > I(0.061) > I(0.057)$ , but has an order of  $I(0.078) > I(0.057) > I(0.082) \approx I(0.061)$ , which does not necessarily imply an inconsistency between Co  $L_{3\text{-edge}}$  XANES and valence-band SPEM data, because delocalization of Co 3d orbitals may spread the Co 3d band into a region deeper than the region of feature  $A_2$ . Delocalization of the Co 3d band for  $x=0.082$  and 0.061 is indicated by the enhancement of the intensities of their spectra relative to that of  $x=0.082$  for binding energies deeper than  $\sim 3.7$  eV.

The difference valence-band spectra between  $\text{Zn}_{1-x}\text{Co}_x\text{O}$  and ZnO nanorods are plotted at the bottom of Fig. 4. The intensities of SPEM features  $A_2$  and  $B_2$  for  $x=0.57$  nanorods are larger than those for  $x=0.061$  and 0.082 nanorods. The intensities of features  $A_2$  and  $B_2$  are enhanced and reduced, respectively, for  $x=0.078$  nanorods relative to those of  $x=0.057$  nanorods. Since a larger intensity of feature  $A_2$  corresponds to more localized Co 3d orbitals and consequently larger Co magnetic moment, the SPEM result suggests that the  $x=0.078$  sample has the largest Co magnetic moment, followed by the  $x=0.057$  sample and both  $x=0.082$  and 0.061 samples have the smallest Co magnetic moment in consistent with that inferred from the XMCD and the magnetization hysteresis loop data. Note that Sato and Katayama-Yoshida in a theoretical study also correlated ferromagnetism in  $\text{Zn}_{1-x}\text{Co}_x\text{O}$  nanorods with high DOSs of Co 3d minority-spin states at/near  $E_F$ .<sup>22</sup>

The combination of Co  $L_{3,2}$ -edge XMCD and valence-band SPEM results shows that the density of the Co 3d states in the vicinity of  $E_F$  plays an important role in the determination of the ferromagnetic property of  $\text{Zn}_{1-x}\text{Co}_x\text{O}$  nanorods. The present result is different from those of Krishnamurthy *et al.*<sup>14</sup> and Venkatesan *et al.* and Coey *et al.*<sup>10</sup> for  $\text{Zn}_{1-x}\text{Co}_x\text{O}$  thin films. They proposed that Co magnetic moments are

closely related to the overlapping of unoccupied TM 3d states with shallow donor states, which lie about 3.2 eV (band gap of ZnO) above VBM. Durst *et al.* argued that defects tend to form bound magnetic polarons that couple with Co 3d moments within its orbits and the overlapping of two similar magnetic polarons induces spin-spin interactions between Co ions, which stabilizes the ferromagnetic ordering in  $\text{Zn}_{1-x}\text{Co}_x\text{O}$  nanorods.<sup>23</sup> The validity of this argument requires relatively long ranged spin polarization of O ions by the defects, which is incompatible with the present observation of the lack of correlation between O  $K$ -edge spectra of  $\text{Zn}_{1-x}\text{Co}_x\text{O}$  nanorods and their magnetic properties as shown in the inset of Fig. 3.

This work was supported by the National Science Council of Taiwan under Contract No. NSC 95-2112-M032-014.

<sup>1</sup>J. K. Furdyna and J. Kossut, *Diluted Magnetic Semiconductors*, Semiconductors and Semimetals Vol. 25 (Academic, New York, 1988).

<sup>2</sup>H. Ohno, *Science* **281**, 951 (1998).

<sup>3</sup>T. Dietl, H. Ohno, F. Matsukura, J. Cibert, and D. Ferrand, *Science* **287**, 1019 (2000).

<sup>4</sup>M. H. Huang, S. Mao, H. Feick, H. Yan, Y. Wu, H. Kind, E. Weber, R. Russo, and P. Yang, *Science* **292**, 1897 (2001).

<sup>5</sup>B. Martinez, F. Sandiumenge, L.I. Balcells, J. Arbiol, F. Sibieude, and C. Monty, *Appl. Phys. Lett.* **86**, 103113 (2005).

<sup>6</sup>J.-H. Kim, J.-H. Park, B.-G. Park, H.-J. Noh, S.-J. Oh, J. S. Yang, D.-H. Kim, S. D. Bu, T.-W. Noh, H.-J. Lin, H.-H. Hsieh, and C. T. Chen, *Phys. Rev. Lett.* **90**, 017401 (2003).

<sup>7</sup>P. V. Radovanovic and D. R. Gamelin, *Phys. Rev. Lett.* **91**, 157202 (2003).

<sup>8</sup>P. Mahadevan, A. Zunger, and D. D. Sarma, *Phys. Rev. Lett.* **93**, 177201 (2004).

<sup>9</sup>C. H. Park and J. D. Chadi, *Phys. Rev. Lett.* **94**, 127204 (2005).

<sup>10</sup>M. Venkatesan, C. B. Fitzgerald, J. G. Lunney, and J. M. D. Coey, *Phys. Rev. Lett.* **93**, 177206 (2004); J. M. D. Coey, M. Venkatesan, and C. B. Fitzgerald, *Nat. Mater.* **4**, 173 (2005).

<sup>11</sup>J. Okabayashi, K. Ono, M. Mizuguchi, M. Oshia, S. S. Gupta, D. D. Sarma, T. Mizokawa, A. Fujimori, M. Yuri, C. T. Chen, T. Fukumura, M. Kawasaki, and H. Koinuma, *J. Appl. Phys.* **95**, 3573 (2004).

<sup>12</sup>S. C. Wi, J. S. Kang, J. H. Kim, S. B. Cho, B. J. Kim, S. Yoon, B. J. Suh, S. W. Han, K. H. Kim, K. J. Kim, B. S. Kim, H. J. Song, H. J. Shin, J. H. Shim, and B. I. Min, *Appl. Phys. Lett.* **84**, 4233 (2004).

<sup>13</sup>S. S. Lee, G. Kim, S. C. Wi, J.-S. Kang, S. W. Han, Y. K. Lee, K. S. An, S. J. Kwon, M. H. Jung, and H. J. Shin, *J. Appl. Phys.* **99**, 08M103 (2006).

<sup>14</sup>S. Krishnamurthy, C. McGuinness, L. S. Dorneles, M. Venkatesan, J. M. D. Coey, J. G. Lunney, C. H. Patterson, K. E. Smith, T. Learmonth, P. A. Glans, T. Schmitt, and J. H. Guo, *J. Appl. Phys.* **99**, 08M111 (2006).

<sup>15</sup>H. J. Lee, S. Y. Jeong, C. R. Cho, and C. H. Park, *Appl. Phys. Lett.* **81**, 4020 (2002).

<sup>16</sup>J. W. Chiou, J. C. Jan, H. M. Tsai, C. W. Bao, W. F. Pong, M.-H. Tsai, I.-H. Hong, R. Klausner, J. F. Lee, J. J. Wu, and S. C. Liu, *Appl. Phys. Lett.* **84**, 3462 (2004).

<sup>17</sup>J. W. Chiou, K. P. Krishna Kumar, J. C. Jan, H. M. Tsai, C. W. Bao, W. F. Pong, F. Z. Chien, M.-H. Tsai, I.-H. Hong, R. Klausner, J. F. Lee, J. J. Wu, and S. C. Liu, *Appl. Phys. Lett.* **85**, 3220 (2004).

<sup>18</sup>J. W. Chiou, H. M. Tsai, C. W. Bao, K. P. Krishna Kumar, S. C. Ray, F. Z. Chien, W. F. Pong, M.-H. Tsai, C. H. Chen, H.-J. Lin, J. J. Wu, M. H. Yang, S. C. Liu, H. H. Chiang, and C. W. Chen, *Appl. Phys. Lett.* **89**, 043121 (2006).

<sup>19</sup>J. J. Wu, S. C. Liu, and M. H. Yang, *Appl. Phys. Lett.* **85**, 1027 (2004).

<sup>20</sup>M. Gruyters, *Phys. Rev. Lett.* **95**, 077204 (2005).

<sup>21</sup>S. J. Hu, S. S. Yan, M. W. Zhao, and L. M. Mei, *Phys. Rev. B* **73**, 245205 (2006).

<sup>22</sup>K. Sato and H. Katayama-Yoshida, *Jpn. J. Appl. Phys., Part 2* **40**, L334 (2001).

<sup>23</sup>A. D. Durst, R. N. Bhatt, and P. A. Wolff, *Phys. Rev. B* **65**, 235205 (2002).

Applied Physics Letters is copyrighted by the American Institute of Physics (AIP). Redistribution of journal material is subject to the AIP online journal license and/or AIP copyright. For more information, see <http://ojps.aip.org/aplo/aplcr.jsp>